Hindawi Publishing Corporation
Journal of Quantum Chemistry
Volume 2014, Article ID 431432, 15 pages
http://dx.doi.org/10.1155/2014/431432

Research Article

A Theoretical Study of the Relationships between Electronic Structure and CB1 and CB2 Cannabinoid Receptor Binding Affinity in a Group of 1-Aryl-5-(1-H-pyrrol-1-yl)-1-H-pyrazole-3-carboxamides

Francisco Salgado-Valdés and Juan S. Gómez-Jeria

Quantum Pharmacology Unit, Department of Chemistry, Faculty of Sciences, University of Chile, Las Palmeras 3425, Nuñoa, 7800003 Santiago, Chile

Correspondence should be addressed to Juan S. Gómez-Jeria; facien03@uchile.cl

Received 31 July 2013; Revised 22 September 2013; Accepted 23 September 2013; Published 2 January 2014

Academic Editor: Daniel Glossman-Mitnik

We report the results of a search for model-based relationships between hCB1 and hCB2 receptor binding affinity and molecular structure for a group of 1-aryl-5-(1-H-pyrrol-1-yl)-1-H-pyrazole-3-carboxamides. The wave functions and local atomic reactivity indices were obtained at the B3LYP/6-31G(d,p) levels of theory with full geometry optimization. Interaction pharmacophores were generated for both receptors. The main conclusions of this work are as follows. (1) We obtained statistically significant equations relating the variation of hCB1 and hCB2 receptor binding affinities with the variation of definite sets of local atomic reactivity indices. (2) The interaction of the molecules with the hCB1 and hCB2 receptors seems to be highly complex and mainly orbital controlled. (3) The interaction mechanisms seem to be different for each type of receptor. This study, contrarily to the statistically backed ones, is able to provide a microscopic insight of the mechanisms involved in the binding process.

1. Introduction

Cannabis has a long history of association with mankind [1]. Probably it was used for medical purposes before recorded history. The cultic use of *Cannabis* seems to have been an extended practice ranging from Rumania east to the Yenisei River from at least the third millennium BC [2–8]. *Cannabis* originated in northern South Asia along the foothills of the Himalayas or the valley of Central Asia. It was first cultivated on a large scale basis in China for fiber and seed production and later in India for resin production. Its cultivation spread from China and India to other places of the world. In 1545 the Spanish brought *Cannabis* to the New World. From the taxonomic point of view, two classes of plants are discernible: a group of plants with relatively limited intoxicant potential, obtained by selection for fiber and oil agronomic qualities, and another group with considerable intoxicant potential, obtained by selection for inebriant qualities. These two groups are classified as subspecies *sativa* and *indica*, of *C. sativa*, the only species of the genus *Cannabis*. Within each subspecies wild and domesticated phases can be recognized. These four groups are recognized as varieties [9–15].

Marijuana consists of a mixture of leaves, stems, and flowering tops of *Cannabis* plants selectively bred to produce high levels of Δ^9-tetrahydrocannabinol (THC or (−)-trans-Δ^9-THC) and several other psychoactive cannabinoids. Various extracts including hashish and hash oil are also produced from the plant. Muslims used *Cannabis* recreationally because alcohol consumption was banned by the Koran. Muslims also introduced hashish, whose popularity spread quickly through 12th century Persia and North Africa. Around 1900 it started to be used as a pleasure-inducing drug in the West [4, 6, 16–20]. It was reported that marijuana

was sometimes used in folk medicine for treating gonorrhea in Sikkim, India [21]. Marijuana's active components are potentially effective in treating pain, nausea, particularly related to cancer chemotherapy, anorexia in AIDS patients, and other conditions such as glaucoma.

The smoke produced by combustion of marijuana contains, among other chemicals, at least sixty-one different cannabinoids. THC produces most of the classical pharmacological effects of smoked marijuana: changes in mood, perception, and motivation. The typical marijuana smoker experiences a high lasting about two hours with impairment of cognitive functions, perception, reaction time, learning, and memory. The pharmacological actions of THC result from its activity at the cannabinoid CB1 receptor, located mainly in the central nervous system, the lungs, liver, and kidneys, and the CB2 receptor, mainly expressed in cells of the immune system and in hematopoietic cells. The protein sequences of CB1 and CB2 receptors are about 44% similar [22–24]. More specifically, the effects of THC are primarily mediated by its activation of CB1 G-protein coupled receptors, which results in a decrease in the concentration of cyclic adenosine monophosphate through the inhibition of adenylate cyclase. The finding of brain cannabinoid receptors led to the discovery of endocannabinoids, such as anandamide and 2-arachidonoyl glyceride [25–28]. Given that both cannabinoid receptors seem to be involved in a great variety of processes the synthesis and testing of new ligands with enhanced activity are still very active lines of research. During the last two decades several families of these ligands have been tested for CB1 and CB2 receptor affinity.

The search for structure-activity relationships (SAR or QSAR) for cannabinoids began during the 1970 decade [29–40]. In a 1987 meeting Mechoulam presented biological data to show that the (−) enantiomers of cannabinoids are more active than the (+) enantiomers [41]. He and collaborators formulated some tentative rules for cannabinomimetic structure-activity relationships, most of them surviving across time. Martin discussed SAR of cannabinoids regarding anticonvulsant activity and Melvin and Johnson presented a review about SAR of tricyclic and nonclassical bicyclic cannabinoids. Their studies demonstrated that some of the analogues exhibited enantiomeric potency. This last study showed that it is possible to achieve extreme biological potency in structures different from the classical cannabinoid ring system (by classical we understand (−)-trans-Δ^9-tetrahydrocannabinol and derivatives). From the quantum-chemical point of view the work by Reggio, presenting the molecular parameters that determine the cannabinomimetic activity, is of great importance [41]. Reggio commented that "traditionally, cannabinoid SARs have been focused almost entirely on the independent contribution of certain structural groups ("functional groups") of the molecules. These SARs have been compiled into extensive "lists of requirements." This type of approach in SAR studies often assumes the following: *that functional groups must react directly with specific sites in the receptor, that modification of one group does not affect the reactivity of another, and that geometric and stereometric factors, such as distance and spatial relationships between functional groups, are all important. Such focus on isolated aspects of the cannabinoids ignores the fact that the molecular properties that are directly responsible for the molecular interactions* (that lead to the pharmacological effect) *are encoded in the entire molecular structure*". This observation is still valid today, not only for cannabinoids but also for all molecules presenting any kind of biological activity. After the discovery of endogenous ligands of CB1 and CB2 receptors and of nonclassical cannabinoids a multitude of structure-activity studies appeared in the literature for the different biological activities of these molecules.

To date, only two quantum-chemical studies carrying out a full characterization of the entire molecules and correlating this characterization with a biological activity have been published in the cannabinoid field [19, 20]. By characterization we mean, in general, a description in quantum-mechanical terms of the reactivity of all atoms constituting the molecule and a representation of the nonelectronic effects of the substituent. A very important condition is that this description must appear in a natural (mathematical) way inside a model linking biological activity with electronic structure (a model-based method). The first paper analyzed the CB1- and CB2-mediated inhibition of adenylyl cyclase by a group of classical cannabinoid derivatives [19]. In the second one we presented structure-receptor affinity relationships for the in vitro interaction of a group of classical (CB1 binding to rat synaptosomal membranes, CB1 binding to African green monkey kidney cells transfected with the cDNA of rat CB1 receptor, and CB2 binding to COS-7 cells transfected with the cDNA of human CB2 receptors), indole-derived (CB1 binding to rat brain P2 membranes), and aminoalkylindole-derived (inhibition of [^{3}H]-WIN-55212-2 binding to rat cerebellar membranes) cannabinoids [20]. From this last work it was concluded that CB1 and CB2 receptor affinities are regulated by different mechanisms involving orbital and charge control. CB1 and CB2 classical ligands share probably three common features: a hydrogen bond to a lysine (for CB1) or serine (for CB2) residue, a fully aromatic ring, and a branched carbon side chain. In the case of indole-derived and aminoalkylindole-derived cannabinoids orientation and alignment rules were defined as a basis for comparison of noncongeneric molecules. In this way it was possible to associate the location of molecular fragments of these systems with known molecular systems such as classical cannabinoids. For aminoalkylindoles we have proposed the locus with which they bind to a second receptor site that is available to WIN-55212-2 but not to classical cannabinoids and anandamide. On the basis of these results a new molecule was proposed that should help to discriminate between the two receptor sites. The results of these studies are very encouraging taking into account that the numerical values for the local atomic descriptors were obtained with a semiempirical method.

On the basis of the already exposed data we have performed here, with more advanced quantum-chemical methods to calculate the electronic structure together with an expanded formal method describing the in vitro drug-receptor interaction, a study relating local atomic reactivity

indices with human recombinant CB1 (hCB1) and CB2 (hCb2) receptor binding affinities in a group of 1-aryl-5-(1H-pyrrol-1-yl)-1H-pyrazole-3-carboxamides [42].

2. Methods, Models, and Calculations

We have developed a formal model to correlate the in vitro drug-receptor affinity constant with the electronic and molecular structure [43–46]. This model has shown, beyond all reasonable doubt, that it can shed light on the fine structure of the drug-receptor interaction ([20, 47–56] and references therein). As the last paper using this model and not belonging to our unit was published in 1979 we shall present in the following part the main lines of its development. Let us consider the state of thermodynamic equilibrium and a 1 : 1 stoichiometry in the formation of the drug-receptor complex:

$$D_i + R \rightleftharpoons D_iR, \tag{1}$$

where D_i is the drug, R is the receptor, and D_iR is the drug-receptor complex. According to statistical thermodynamics the equilibrium constant, K_i, is expressed as

$$K_i = \frac{Q_{D_iR}}{Q_{D_i}Q_R} \exp\left(-\frac{\Delta\varepsilon_0^i}{kT}\right), \tag{2}$$

where $\Delta\varepsilon_0^i$ is the difference between the ground-state energy of D_iR and the energies of the ground states of D_i and R:

$$\Delta\varepsilon_0^i = \varepsilon_{D_iR} - \left(\varepsilon_{D_i} + \varepsilon_R\right) \tag{3}$$

and the Q's are the total partition functions (PFs) measured from the ground state (in solution). T and k are the temperature and the Boltzmann constant, respectively. If we consider that for practically all polyatomic molecules the Boltzmann factors of the excited electronic states are negligible compared to those of the ground state, that the rotational and vibrational motions are independent and uncoupled, and that at body temperature the vibrational PFs have a value close to 1, and using the classical expression for the rotational PF together with the assumption that the rotational PFs of the receptor and the drug-receptor are similar (this requires that the receptor molecule be much greater than the drug molecule), we may write (2) as [44, 45]

$$\log K_i = a + bM_{D_i} + c\log\left[\frac{\sigma_{D_i}}{(ABC)^{1/2}}\right] + d\Delta\varepsilon_i, \tag{4}$$

where a, b, c, and d are constants, M the drug's mass, σ its symmetry number, and ABC the product of the drug's moment of inertia about the three principal axes of rotation.

The interaction energy $\Delta\varepsilon_i$ cannot be calculated directly due to the size of the receptor. But, as we are dealing with a weak drug-receptor interaction, we can employ the perturbation theory in the Klopman-Hudson form to evaluate $\Delta\varepsilon_i$ [57–59]. According to this method, the change in electron energy, $\Delta\varepsilon$, associated with the interaction of atoms i and j is [45]

$$\Delta\varepsilon = \sum_p \left[\frac{Q_iQ_j}{R_{ij}} + \left(\frac{1}{2}\right)\left(\beta_{ij}^2\right)\sum_m\sum_n \frac{F_{mi}F_{n'j}}{(E_m - E_{n'})} - \left(\frac{1}{2}\right)\left(\beta_{ij}^2\right)\sum_m\sum_{n'} \frac{F_{m'i}F_{nj}}{(E_{m'} - E_n)}\right], \tag{5}$$

where Q_i is the net charge of atom i, F_{mi} is the Fukui index of atom i in the MO m (i.e., the electron population per MO and per atom) [60], β_{ij} is the resonance integral, and $E_m(E_{m'})$ is the energy of the mth (m'th) occupied (virtual) MO of molecule A, with n and n' standing for molecule B. The value of β_{ij} is kept independent of the kind of AO because the drug-receptor complex does not involve covalent bonds. The summation on p is over all pairs of interacting atoms of the drug and the receptor. The first term of the right side of (5) represents the electrostatic interaction between two atoms having net charges Q_i and Q_j. The second and third terms introduce the interactions between the occupied and empty MOs of the drug and those of the receptor. Recent working on the expression for $\Delta\varepsilon$ allowed us to include local atomic reactivity indices coming from the density functional theory (DFT) [46, 61]. The final expression for $\Delta\varepsilon$ is

$$\begin{aligned}\Delta\varepsilon \cong{}& \sum_j \left[e_jQ_j + f_jS_j^E + s_jS_j^N\right] \\ &+ \sum_j\sum_m \left[h_j(m)F_j(m) + x_j(m)S_j^E(m)\right] \\ &+ \sum_j\sum_{m'} \left[r_j\left(m'\right)F_j\left(m'\right) + t_j\left(m'\right)S_j^N\left(m'\right)\right] \\ &+ \sum_j \left[g_j\mu_j + k_j\eta_j + o_j\omega_j + z_j\varsigma_j + w_jQ_j^{\max}\right],\end{aligned} \tag{6}$$

where S_j^E and S_j^N are, respectively, the total atomic electrophilic (TAESD) and nucleophilic (TANSD) superdelocalizabilities of atom j, $S_j^E(m)$ is the electrophilic superdelocalizability of atom j at occupied MO m, and $S_j^N(m')$ is the nucleophilic superdelocalizability of atom j at empty MO m' [60]. TAESD is simply the sum over all occupied MOs of $S_j^E(m)$ and TANSD is the sum over all empty MOs of $S_j^N(m')$. These indices are very helpful to compare the reactivity of similar atomic positions through a series of molecules because they include the eigenvalue spectrum which is habitually different in each molecular system. The last bracket of the right side of (6) contains the new local atomic reactivity indices. μ_i, η_i, ω_i, ς_i, and $Q_i^{\max}$ are, respectively, the local atomic electronic chemical potential of atom i, the local atomic hardness of atom i, the local electrophilicity of atom i, the local atomic softness of atom i, and the maximal quantity of electronic charge atom i can receive (for the mathematical definitions of the indices see [46]). For the sake of clarity we present in Table 1 a summary of these local atomic reactivity indices (LARIs) together with their physical meaning. Some

of these new indices have appeared in recent QSAR studies [56, 62].

The insertion of (6) into (4) leads to master equation (7):

$$\begin{aligned}\log K_i &= a + bM_{D_i} + c\log\left[\frac{\sigma_{D_i}}{(ABC)^{1/2}}\right] + \sum_j \left[e_j Q_j + f_j S_j^E + s_j S_j^N\right] \\ &+ \sum_j \sum_m \left[h_j(m) F_j(m) + x_j(m) S_j^E(m)\right] \\ &+ \sum_j \sum_{m'} \left[r_j(m') F_j(m') + t_j(m') S_j^N(m')\right] \\ &+ \sum_j \left[g_j \mu_j + k_j \eta_j + o_j \omega_j + z_j \varsigma_j + w_j Q_j^{\max}\right].\end{aligned} \tag{7}$$

The moment of inertia term is a whole molecular property. It was shown that it can be expressed in a first approximation as [51, 63]

$$\log\left[(ABC)^{-1/2}\right] = \sum_t \sum_t m_{i,t} R_{i,t}^2 = \sum_t O_t, \tag{8}$$

where the summation over t is over the different substituents of the molecule and $m_{i,t}$ is the mass of the ith atom belonging to the tth substituent, with $R_{i,t}$ being its distance to the atom to which the substituent is attached. We have called them orientation parameters. Equation (8) transformed a molecular property into a sum of local properties. We have interpreted these orientational parameters as follows. The bioactive molecules are moving inside a biological fluid. Inside this fluid, accumulation, recognition, and guiding of the drug molecule toward the receptor through long-range interactions occur. In order to interact with the receptor, a time interval τ is required, in which the molecule must attain a given rotational velocity. Only below this velocity value will the receptor molecular electrostatic potential (MEP) have time to match the drug MEP to guide it and to engage in short-range interactions. Within this reasoning scheme we interpret (8) (because it comes from the rotational partition function) as accounting for the relative ease with which this process occurs.

Then, for n molecules we have a system of n linear equations. In principle, this system of simultaneous equations holds for all the atoms of the drug directly perturbed by their interaction with the receptor. Combined with multiple-regression techniques, these equations can be usefully applied to estimate the relative variation of $\log K_i$ in a family of molecules. Also, they can be used to determine which atoms are directly concerned in the formation of the drug-receptor complex. Here statistical analysis is used, *not to see whether there is a structure-activity relationship but to find the best one*.

The most important attribute of the master equation is that it contains terms associated only to the drug molecule. Note also that the numerical values of the LARIs can be obtained with any quantum-chemical calculation (semiempirical, *ab initio* or DFT). This equation, in its older and present forms, produced good results for very diverse drug-receptor systems [20, 47, 49–56, 62, 64, 65].

Table 1: Local atomic reactivity indices and their meaning.

LARI	Name	Physical meaning
Q_i	Net atomic charge of atom i	Electrostatic interaction
S_i^E	Total atomic electrophilic superdelocalizability of atom i	Total atomic electron-donating capacity of atom i (MO-MO interaction)
S_i^N	Total atomic nucleophilic superdelocalizability of atom i	Total atomic electron-accepting capacity of atom i (MO-MO interaction)
$S_i^E(m)$	Orbital atomic electrophilic superdelocalizability of atom i and occupied MO m	Electron-donating capacity of atom i at occupied MO m (MO-MO interaction)
$S_i^N(m')$	Orbital atomic nucleophilic superdelocalizability of atom i and empty MO m'	Electron-accepting capacity of atom i at empty MO m' (MO-MO interaction)
F_i	Fukui index of atom i	Total electron population of atom i (MO-MO interaction)
F_{mi}	Fukui index of atom i and occupied MO m	Electron population of occupied MO m at atom i (MO-MO interaction)
$F_{m'i}$	Fukui index of atom i and empty MO m'	Electron population of empty MO m' at atom i (MO-MO interaction)
μ_i	Local atomic electronic chemical potential of atom i	Propensity of atom i to gain or lose electrons
η_i	Local atomic hardness of atom i	Resistance of atom i to exchange electrons with the environment
ς_i	Local atomic softness of atom i	The inverse of η_i
ω_i	Local atomic electrophilicity of atom i	Predisposition of atom i to receive extra electronic charge together with its resistance to exchange charge with the medium
$Q_i^{\max}$	Maximal amount of electronic charge atom i may receive	Maximal amount of electronic charge that atom i may receive

The molecules chosen for this study are shown in Figure 1 and Table 2, together with the corresponding experimental receptor binding affinities. Geometries were fully optimized at the B3LYP/6-31G(d,p) level of the theory with the Gaussian98 suite of programs [66]. With software written in our laboratory we extracted from the Gaussian results all the necessary information to obtain numerical values for the LARIs. All electron populations smaller than or equal to 0.01 e were considered as zero [46]. Negative electron populations

Table 2: Molecules and their experimental binding affinities.

Molecule	R1	R1′	R1″	R2	R3	R3′	log *k* (hCB1)	log *k* (hCB2)
1	-Cl	-Cl	-H	4-Chlorophenyl	-H	-H	2.08	1.90
2	-Cl	-Cl	-H	4-Chlorobenzyl	-H	-H	2.15	2.97
3	-Cl	-Cl	-H	2-Bromo-3,4,5-trimethoxybenzyl	-H	-H	2.36	—
4	-Cl	-Cl	-H	(4-Chlorophenyl)ethyl	-H	-H	1.85	—
5	-Cl	-Cl	-H	(3,4-Dichlorophenyl)ethyl	-H	-H	2.20	—
6	-Cl	-Cl	-H	(3-Chloro-4-methoxyphenyl)ethyl	-H	-H	2.57	3.46
7	-Cl	-Cl	-H	(2,4-Dichlorophenyl)ethyl	-H	-H	2.34	—
8	-Cl	-Cl	-H	Cyclopentyl	-H	-H	1.92	2.23
9	-Cl	-Cl	-H	Cycloheptyl	-H	-H	1.30	1.30
10	-Cl	-Cl	-H	4-Chlorophenyl	-Me	-Me	1.98	—
11	-Cl	-Cl	-H	4-Chlorobenzyl	-Me	-Me	1.95	—
12	-Cl	-Cl	-H	2-Bromo-3,4,5-trimethoxybenzyl	-Me	-Me	2.16	2.74
13	-Cl	-Cl	-H	(4-Chlorophenyl)ethyl	-Me	-Me	1.48	—
14	-Cl	-Cl	-H	(3,4-Dichlorophenyl)ethyl	-Me	-Me	2.07	—
15	-Cl	-Cl	-H	(3-Chloro-4-methoxyphenyl)ethyl	-Me	-Me	2.05	3.54
16	-Cl	-Cl	-H	(2,4-Dichlorophenyl)ethyl	-Me	-Me	2.19	—
17	-Cl	-Cl	-H	Cyclopentyl	-Me	-Me	2.18	2.49
18	-Cl	-Cl	-H	Cycloheptyl	-Me	-Me	1.90	1.90
19	-H	-Cl	-Cl	4-Chlorophenyl	-H	-H	3.11	2.90
20	-H	-Cl	-Cl	4-Chlorobenzyl	-H	-H	1.85	2.00
21	-H	-Cl	-Cl	(4-Chlorophenyl)ethyl	-H	-H	2.38	3.08
22	-H	-Cl	-Cl	Cyclopentyl	-H	-H	1.70	1.08
23	-H	-Cl	-Cl	Cycloheptyl	-H	-H	0.75	0.11
24	-H	-Cl	-Cl	Adamant-1-yl	-H	-H	1.49	1.30
25	-H	-Cl	-Cl	4-Chlorobenzyl	-Me	-Me	2.00	2.90
26	-H	-Cl	-Cl	(4-Chlorophenyl)ethyl	-Me	-Me	2.59	—
27	-H	-Cl	-Cl	Cyclopentyl	-Me	-Me	1.56	1.08
28	-H	-Cl	-Cl	Cycloheptyl	-Me	-Me	1.08	0.62
29	-H	-Cl	-Cl	Adamant-1-yl	-Me	-Me	0.75	1.08
30	-F	-F	-H	4-Chlorophenyl	-H	-H	3.32	—
31	-F	-F	-H	4-Chlorobenzyl	-H	-H	2.53	3.53
32	-F	-F	-H	2-Bromo-3,4,5-trimethoxybenzyl	-H	-H	2.54	—
33	-F	-F	-H	(4-Chlorophenyl)ethyl	-H	-H	1.90	—
34	-F	-F	-H	(3,4-Dichlorophenyl)ethyl	-H	-H	2.49	3.11
35	-F	-F	-H	(3-Chloro-4-methoxyphenyl)ethyl	-H	-H	2.98	3.29
36	-F	-F	-H	(2,4-Dichlorophenyl)ethyl	-H	-H	2.58	2.82
37	-F	-F	-H	Cyclopentyl	-H	-H	3.38	3.04
38	-F	-F	-H	Cycloheptyl	-H	-H	2.75	2.30
39	-F	-F	-H	4-Chlorophenyl	-Me	-Me	2.75	—
40	-F	-F	-H	4-Chlorobenzyl	-Me	-Me	1.75	—
41	-F	-F	-H	2-Bromo-3,4,5-trimethoxybenzyl	-Me	-Me	2.22	—

Table 2: Continued.

Molecule	R1	R1′	R1″	R2	R3	R3′	log k (hCB1)	log k (hCB2)
42	-F	-F	-H	(4-Chlorophenyl)ethyl	-Me	-Me	1.70	—
43	-F	-F	-H	(3,4-Dichlorophenyl)ethyl	-Me	-Me	1.73	—
44	-F	-F	-H	(3-Chloro-4-methoxyphenyl)ethyl	-Me	-Me	2.00	—
45	-F	-F	-H	(2,4-Dichlorophenyl)ethyl	-Me	-Me	1.61	2.86
46	-F	-F	-H	Cyclopentyl	-Me	-Me	2.92	2.95
47	-F	-F	-H	Cycloheptyl	-Me	-Me	1.75	2.04

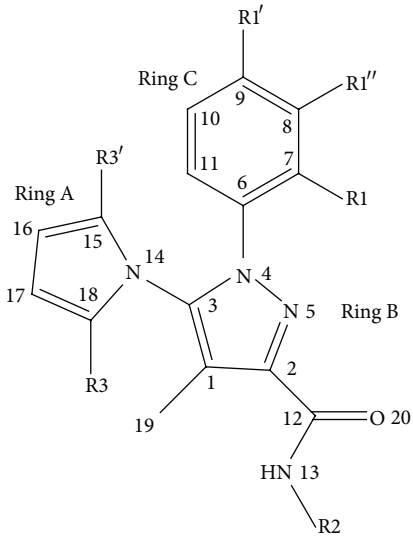

Figure 1: General formula of the molecules analyzed in this study. Numbers refer to the common skeleton used for LMRA.

coming from the mulliken population analysis were corrected according to a recent proposed method [67]. Here we shall work with the common skeleton hypothesis which states that there is a definite group of atoms, common to all molecules analyzed, in which the variation of their electronic properties accounts for nearly all the variation of the biological activity through the series. Implicit in this choice is the supposition that this common skeleton is aligned, in all molecules, in almost the same position to interact with the receptor. The effects of the substituents consist in modifying the electronic structure of this common skeleton. For the case studied here the common skeleton numbering is shown in Figure 1 (atoms 1–20).

All the linear multiple regression analyses (LMRA) were performed with the Statistica software [68]. The dependent variable is the logarithm of the corresponding biological activity [42] and the independent variables are the local atomic reactivity indices of the common skeleton plus the orientational parameters of the substituents R1, R′1, R″1, R_2, R_3, and R′3 (see Figure 1). The orientational parameters were calculated as usual [51, 63].

For a clear understanding of the results we need to comment on the formation of the matrix containing the variables. Figure 2 shows an example for three atoms, I, II, and III, and for the three upper occupied and three lowest empty molecular orbitals (this figure was previously used, [46, 56, 61]).

If we include in an initial data matrix all electron populations (the Fukui indices), we get the one shown in the upper side of (9). But the interactions between the drug and the receptor are achieved only through nonzero electron populations. Therefore the actual matrix for Figure 2 is the one shown in the middle side of (9). Then for atom I its HOMO, HOMO − 1, LUMO, and LUMO + 1 match with the corresponding molecular orbitals, but for atoms II and III this is not the case. To avoid misunderstandings we have used the nomenclature depicted at the lower side of (9). Here, for example, $F_i(\mathrm{HOMO}-1)^*$ refers to the first highest MO having a nonzero electron population at atom i.

Matrix building for independent variables is as follows:

$$\begin{Bmatrix} \mathrm{I} & & \mathrm{II} & & \mathrm{III} \\ F_i(\mathrm{L}+1) & \cdots & F_i(\mathrm{L}+1) & \cdots & F_i(\mathrm{L}+1) \\ F_i(\mathrm{L}) & \cdots & F_i(\mathrm{L}) & \cdots & F_i(\mathrm{L}) \\ F_i(\mathrm{H}) & \cdots & F_i(\mathrm{H}) & \cdots & F_i(\mathrm{H}) \\ F_i(\mathrm{H}-1) & \cdots & F_i(\mathrm{H}-1) & \cdots & F_i(\mathrm{H}-1) \end{Bmatrix}$$

$$\longrightarrow \begin{Bmatrix} \mathrm{I} & & \mathrm{II} & & \mathrm{III} \\ F_i(\mathrm{L}+1) & \cdots & F_i(\mathrm{L}+2) & \cdots & F_i(\mathrm{L}+2) \\ F_i(\mathrm{L}) & \cdots & F_i(\mathrm{L}) & \cdots & F_i(\mathrm{L}+1) \\ F_i(\mathrm{H}) & \cdots & F_i(\mathrm{H}) & \cdots & F_i(\mathrm{H}-1) \\ F_i(\mathrm{H}-1) & \cdots & F_i(\mathrm{H}-2) & \cdots & F_i(\mathrm{H}-2) \end{Bmatrix}$$

$$\longrightarrow \begin{Bmatrix} \mathrm{I} & & \mathrm{II} & & \mathrm{III} \\ F_i(\mathrm{L}+1)^* & \cdots & F_i(\mathrm{L}+1)^* & \cdots & F_i(\mathrm{L}+1)^* \\ F_i(\mathrm{L})^* & \cdots & F_i(\mathrm{L})^* & \cdots & F_i(\mathrm{L})^* \\ F_i(\mathrm{H})^* & \cdots & F_i(\mathrm{H})^* & \cdots & F_i(\mathrm{H})^* \\ F_i(\mathrm{H}-1)^* & \cdots & F_i(\mathrm{H}-1)^* & \cdots & F_i(\mathrm{H}-1)^* \end{Bmatrix}. \quad (9)$$

3. Results

3.1. hCB1 Receptor Binding Affinity. The first LMRA carried out with the whole set ($n = 47$) showed that the standard residual of molecule 23 fell outside the $\pm 2\sigma$ limit. A second LMRA excluding this case ($n = 46$) led to an equation with a standard error of the estimate (SD) of 0.38 and explaining only 53% of the variation of CB1 receptor binding affinity through the series. This suggested immediately that the common skeleton working hypothesis could not be entirely right for the whole set and that perhaps some of the molecule's

Table 3: Beta coefficients and t-test for significance of coefficients in (10).

	Beta	t (24)	P level
S_8^N (LUMO + 2)*	−0.75	−9.10	<0.0000001
S_{19}^E (HOMO − 1)*	0.34	3.49	<0.002
S_1^N (LUMO + 2)*	0.33	3.70	<0.001
F_{20} (HOMO − 2)*	−0.33	−3.75	<0.001
F_{16} (HOMO − 2)*	−0.22	−2.77	<0.01

substituents also bind directly to another area of the receptor. Examination of Table 2 shows that some R2 substituents have π electrons while others do not. Therefore we build two separate sets, one containing the R2 substituents with π electrons (Set I, $n = 33$) and the other containing only fully saturated R2 substituents (Set II, $n = 14$).

For the case of Set I preliminary LMRAs showed that molecules 11, 15, and 25 displayed standard residuals outside the $\pm 2\sigma$ limit. Discarding these cases we obtained the following regression equation:

$$\begin{aligned}\log k\,(\text{hCB1}) &= 2.45 - 0.04S_8^N(\text{LUMO}+2)^* + 3.49S_{19}^E(\text{HOMO}-1)^* \\ &\quad + 0.002S_1^N(\text{LUMO}+2)^* - 0.36F_{20}(\text{HOMO}-2)^* \\ &\quad - 0.71F_{16}(\text{HOMO}-2)^*\end{aligned} \tag{10}$$

with $n = 30$, $R = 0.93$, adj $R^2 = 0.86$, $F(5, 24) = 29.802$ ($P < 0.000001$), outliers $> 2\sigma = 0$, and SD $= 0.16$. Here $S_8^N(\text{LUMO}+2)^*$ and $S_1^N(\text{LUMO}+2)^*$ refer, respectively, to the LUMO + 2 nucleophilic superdelocalizability of atoms 8 and 1; $S_{19}^E(\text{HOMO}-1)^*$ is the electrophilic superdelocalizability of HOMO − 1 at atom 19; $F_{20}(\text{HOMO}-2)^*$ and $F_{16}(\text{HOMO}-2)^*$ are the Fukui indices of the HOMO − 2 at atoms 20 and 16, respectively. The beta coefficients and t-test for significance of coefficients of (10) are shown in Table 3. Concerning independent variables, Table 4 shows that there are no significant internal correlations at $P < 0.05$. Figure 3 shows the plot of observed values versus calculated ones. No outliers were detected and no residuals fall outside the $\pm 2\sigma$ limits. The associated statistical parameters of (10) show that this equation is statistically significant, explaining about 86% of the variation of the hCB1 receptor binding affinity.

For the case of Set II the best equation obtained was

$$\begin{aligned}\log k\,(\text{hCB1}) &= 10.73 + 1.09S_5^E(\text{HOMO}-2)^* - 10.03Q_8^{\max} \\ &\quad - 37.63F_{19}(\text{HOMO}-2)^* - 0.0006\Phi_{\text{R1}}\end{aligned} \tag{11}$$

with $n = 14$, $R = 0.98$, adj $R^2 = 0.95$, $F(4, 9) = 69.67$ ($P < 0.000001$), outliers $> 2\sigma = 0$, and SD $= 0.17$. Here, Φ_{R1} is the orientational effect of the R1 substituent, $S_5^E(\text{HOMO}-2)^*$ is the HOMO − 2 electrophilic superdelocalizability at atom 5, $F_{19}(\text{HOMO}-2)^*$ is the Fukui index of HOMO − 2 at atom 19, and $Q_8^{\max}$ is the maximal amount of charge that atom 8 may accept. The beta coefficients and t-test for significance of coefficients of (11) are shown in Table 5. Concerning independent variables, Table 6 shows that there are no significant internal correlations at $P < 0.05$. Figure 4 shows the plot of observed values versus calculated ones. No outliers were detected and no residuals fall outside the $\pm 2\sigma$ limits. The associated statistical parameters of (11) show that this equation is statistically significant, explaining about 95% of the variation of the hCB1 receptor binding affinity.

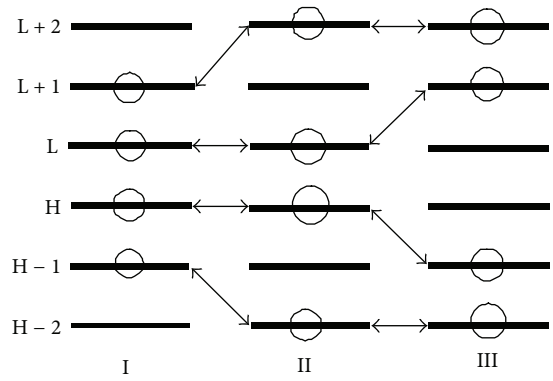

Figure 2: Molecular orbitals and electronic populations (Fukui indices). H means HOMO (the highest occupied MO), H − 1 the next upper occupied MO, H−2 the second next upper occupied MO, L the LUMO (the lowest unoccupied MO), L + 1 the second lowest unoccupied MO, and L + 2 the third lowest unoccupied MO. The circles depict those MOs in which an atom has a nonzero electron population.

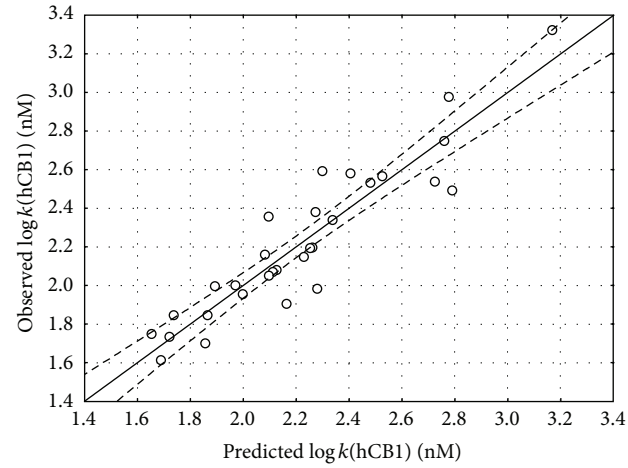

Figure 3: Observed versus calculated values (10) of $\log k$(hCB1). Dashed lines denote the 95% confidence interval.

3.2. hCB2 Receptor Binding Affinity. The first LMRA carried out with the whole set ($n = 31$) indicated that the standard residual of molecule 15 fell outside the $\pm 2\sigma$ limit. A second LMRA excluding this case ($n = 30$) led to an equation with a standard error of the estimate of 0.29 and explaining only 87% of the variation of CB2 receptor binding affinity throughout the series. For these reasons we proceeded as in the case

Table 4: Squared correlation coefficients for the variables appearing in (10).

	S_1^N (LUMO + 2)*	S_8^N (LUMO + 2)*	F_{16} (HOMO − 2)*	S_{19}^E (HOMO − 1)*
S_8^N (LUMO + 2)*	0.12	1.00		
F_{16} (HOMO − 2)*	0.006	0.02	1.00	
S_{19}^E (HOMO − 1)*	0.17	0.02	0.08	1.00
F_{20} (HOMO − 2)*	0.03	0.005	0.0009	0.2

Table 5: Beta coefficients and t-test for significance of coefficients in (11).

	Beta	t (10)	P-level
S_5^E (HOMO − 2)*	0.28	3.90	<0.004
$Q_8^{\max}$	−0.74	−11.05	<0.000002
F_{19} (HOMO − 2)*	−0.38	−5.75	<0.0003
Φ_{R1}	−0.29	−4.52	<0.001

Table 6: Squared correlation coefficients for the variables appearing in (11).

	S_5^E (HOMO − 2)*	$Q_8^{\max}$	F_{19} (HOMO − 2)*
$Q_8^{\max}$	0.19	1.00	
F_{19} (HOMO − 2)*	0.14	0.07	1.00
Φ_{R1}	0.10	0.06	0.004

Table 7: Beta coefficients and t-test for significance of coefficients in (12).

	Beta	t (12)	P-level
S_{17}^N (LUMO)*	0.70	13.29	0.0000001
F_4 (LUMO + 1)*	0.35	5.75	0.0001
F_{20} (LUMO + 2)*	−0.48	−8.64	0.000003
F_{19} (LUMO + 2)*	−0.20	−3.54	0.005
Q_{19}	−0.17	−3.18	0.009

of CB1 data and formed Set III comprising those molecules with an R2 substituent with π electrons ($n = 17$) and Set IV containing only fully saturated R2 substituents ($n = 14$).

For Set III the best equation obtained was

$$\begin{aligned}\log k\,(\text{hCB2}) &= 1.42 + 0.03S_{17}^N(\text{LUMO})^* + 3.02F_4(\text{LUMO}+1)^* \\ &\quad - 3.63F_{20}(\text{LUMO}+2)^* \\ &\quad - 1.30F_{19}(\text{LUMO}+2)^* - 4.07Q_{19}\end{aligned} \tag{12}$$

with $n = 17$, $R = 0.98$, adj $R^2 = 0.96$, $F(5, 11) = 87.86$ ($P < 0.000001$), outliers $> 2\sigma = 0$, and SD = 0.09. Here, Q_{19} is the net charge of atom 19, $S_{17}^N(\text{LUMO})^*$ is the local atomic nucleophilic superdelocalizability of atom 17 at the lowest unoccupied MO, and $F_4(\text{LUMO}+1)^*$ is the Fukui index of LUMO + 1 MO at atom 4 with $F_{19}(\text{LUMO}+2)^*$ and $F_{20}(\text{LUMO}+2)^*$ being the Fukui indices of the LUMO + 2 MO at atoms 19 and 20. The beta coefficients and t-test for significance of coefficients of (12) are shown in Table 7. Concerning independent variables, Table 8 shows that there are no significant internal correlations at $P < 0.05$. Figure 5 shows the plot of observed values versus calculated ones. No outliers were detected and no residuals fall outside the $\pm 2\sigma$ limits. The associated statistical parameters of (12) show that this equation is statistically significant, explaining about 96% of the variation of the hCB2 receptor binding.

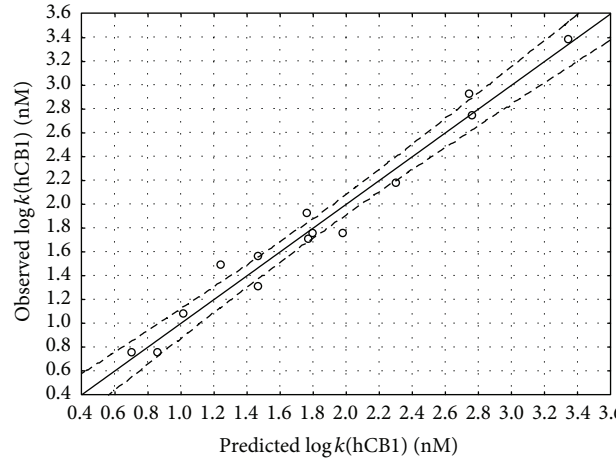

Figure 4: Observed versus calculated values (11) of $\log k$(hCB1). Dashed lines denote the 95% confidence interval.

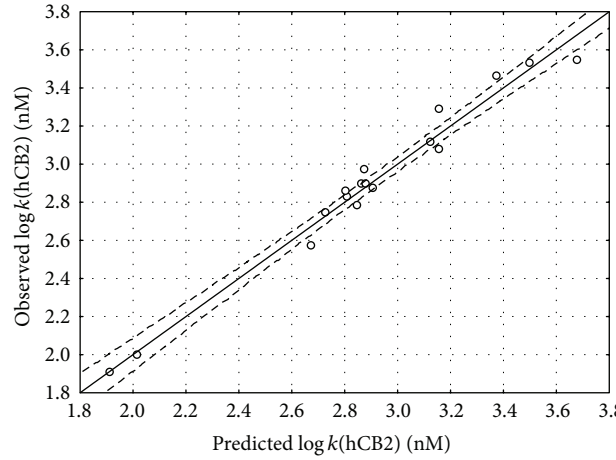

Figure 5: Observed versus calculated values (12) of $\log k$(hCB2). Dashed lines denote the 95% confidence interval.

For Set IV the best statistical equation is

$$\begin{aligned}\log k\,(\text{hCB2}) &= 25.82 - 158.42\mu_{12} - 0.0009\Phi_{R2} \\ &\quad - 52.68F_{12}(\text{HOMO})^* - 4.60S_{18}^E(\text{HOMO}-1)^*\end{aligned} \tag{13}$$

Table 8: Squared correlation coefficients for the variables appearing in (12).

	F_4 (LUMO + 1)*	S^N_{17} (LUMO)*	Q_{19}	F_{19} (LUMO + 2)*
S^N_{17} (LUMO)*	0.05	1.00		
Q_{19}	0.05	0.05	1.00	
F_{19} (LUMO + 2)*	0.16	0.07	0.002	1.00
F_{20} (LUMO + 2)*	0.06	0.02	0.03	0.04

Table 9: Beta coefficients and t-test for significance of coefficients in (13).

	Beta	t (10)	P-level
μ_{12}	0.78	10.46	<0.000002
Φ_{R2}	−0.43	−4.63	<0.001
F_{12} (HOMO)*	−0.26	−2.82	<0.02
S^E_{18} (HOMO − 1)*	−0.19	−2.49	<0.03

Table 10: Squared correlation coefficients for the variables appearing in (13).

	F_{12} (HOMO)*	μ_{12}	S^E_{18} (HOMO − 1)*	Φ_{R2}
F_{12} (HOMO)*	1.00			
μ_{12}	0.02	1.00		
S^E_{18} (HOMO − 1)*	0.004	0.08	1.00	
Φ_{R2}	0.38	0.04	0.03	1.00

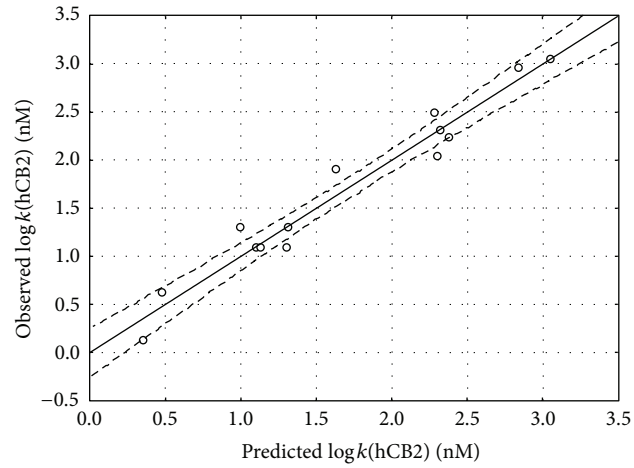

Figure 6: Observed versus calculated values (13) of log k(hCB2). Dashed lines denote the 95% confidence interval.

with $n = 14$, $R = 0.98$, adj $R^2 = 0.94$, $F(4, 9) = 48.24$ ($P < 0.000001$), outliers $> 2\sigma = 0$, and SD $= 0.22$. Here, Φ_{R2} is the orientational parameter of R2 substituent, μ_{12} is the local atomic electronic chemical potential of atom 12, F_{12}(HOMO)* is the Fukui index of the HOMO at atom 12, and S^E_{18}(HOMO − 1)* is the local atomic electrophilic superdelocalizability of HOMO − 1 MO at atom 18. The beta coefficients and t-test for significance of coefficients of (13) are shown in Table 9. Concerning independent variables, Table 10 shows that there are no significant internal correlations at $P < 0.05$. Figure 6 shows the plot of observed values versus calculated ones. No outliers were detected and no residuals fall outside the $\pm 2\sigma$ limits. The associated statistical parameters of (13) show that this equation is statistically significant, explaining about 94% of the variation of the hCB2 receptor binding affinity.

4. Discussion

Before discussing the LRMA results we shall comment on the electronic structure of the molecules studied here, using molecules 1 and 9 as examples. The only difference between them is the nature of the R2 substituent (i.e., molecule 1 has an aromatic R2 substituent and molecule 6 a saturated one). Figure 7 shows the molecular electrostatic potential (MEP) of both molecular systems. The R2 substituent is located at the right side in both images. In molecule 1 a region of negative MEP surrounds almost all the R2 substituent while in molecule 9 the R2 substituent is laying inside of a region of positive MEP. Given the variety of

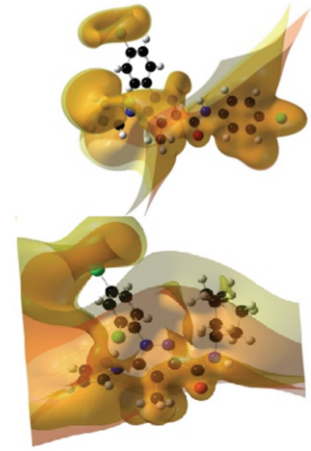

Figure 7: MEP of molecules 1 (upper) and 6 (lower). The orange isovalue surface corresponds to negative MEP values (−0.0004) and the yellow isovalue surface to positive MEP values (0.0004).

R2 substituents (see Table 2) it could be logical to assume that the recognition area could be the left side of these molecules. This question is difficult to answer in a definitive way because of the conformational flexibility of these systems. We employed the fully optimized geometry to obtain the MEP values, but there is no perfect way to know how the conformation (and therefore the MEP's structure) of any of these molecules evolves when they approach the receptor (at body temperature all conformations up to 7 Kcal/mol from

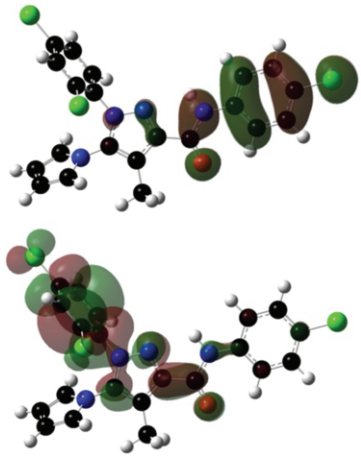

Figure 8: Localization of the HOMO (upper) and LUMO (lower) in molecule 1 (isovalue = 0.02 e).

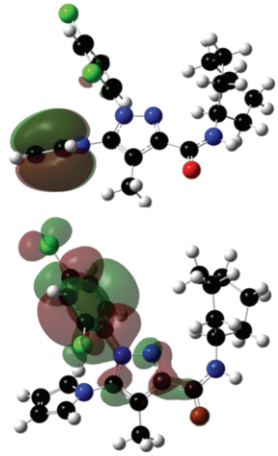

Figure 9: Localization of the HOMO (upper) and LUMO (lower) in molecule 6 (isovalue = 0.02 e).

the fully optimized structure are available). For smaller and almost rigid molecules, such as mescaline derivatives, this can be done with confidence [69].

Another important point to comment on is the localization of the frontier molecular orbitals (HOMO and LUMO). Figure 8 shows the HOMO and LUMO of molecule 1. The HOMO is localized on the R2 substituent while the LUMO is localized mainly on Ring C. This indicates to us that for molecule 1 all electron populations for the HOMO (i.e., F_k(HOMO)) of the common skeleton atoms are zero. Then, if the common skeleton interacts with the receptor through a π molecular orbital, it will do it using an inner π MO. This is a specific example in which the HOMO* of any atom of the common skeleton does not coincide with the molecular HOMO and helps understand the logic underlying the building of the matrix of independent variables to employ in the LMRA. Figure 9 shows the HOMO and LUMO of molecule 6. In this case the HOMO is localized on Ring A (i.e., on the common skeleton) and the LUMO on Ring C as in molecule 1. In this case only the electron populations (the Fukui indices) of Ring A have nonzero values. If this molecule interacts with the receptor through a π molecular orbital localized on Ring A, it will do it using the molecular π HOMO, which is not the case of molecule 1. Note that the LUMOs of molecules 1 and 6 are localized on the same areas.

4.1. hCB1 Receptor Binding Results. When scientists publish a paper containing the synthesis and biological activity of a family of molecules, they normally present a list of requirements with statements such as "when we change this substituent by this other activity diminishes," or similar ones. This is presented normally as QSAR or SAR analysis, but we maintain that this is not strictly the case. Statements of this kind could be right only in the cases when, for example, we replace a chlorine atom by a bromine atom or a methyl group by an ethyl one. Below we shall employ a variable-by-variable (VBV) analysis, but we must not forget that it is the simultaneous variation of all variables in the statistical equation that gives an account of the variation of the biological activity through the family of molecules.

The associated indices of (10) (Set I, aromatic R2 substituents) indicate that this equation is statistically significant. The results show that the variation of log(hCB1) is associated with the variation of several local atomic reactivity indices located at atoms 1, 8, 16, 19, and 20 of the common skeleton (see Figure 1). Table 3 shows that the most important variable is the (LUMO + 2)* nucleophilic superdelocalizability of atom 8 (S_8^N(LUMO + 2)*), followed by the electrophilic superdelocalizability of (HOMO − 1)* at atom 19, the (LUMO + 2)* nucleophilic superdelocalizability of atom 1, and the Fukui index (i.e., the electron population) of the (HOMO − 2)* at atom 20 and F_{16}(HOMO − 2)*. The VBV analysis indicates that a good receptor binding affinity is associated with high values of S_{19}^E(HOMO − 1)*, F_{20}(HOMO − 2)*, and F_{16}(HOMO − 2)*, with small values for S_8^N(LUMO + 2)* and with a negative value for S_1^N(LUMO + 2)*. Let us examine the case of S_1^N(LUMO + 2)*. *Ab initio* and DFT calculations produce most of the time negative eigenvalues for one or more empty MOs. Given that we are analyzing a family of molecules we shall interpret these negative eigenvalues as being relatively more reactive than the upper ones. As the LMRA matrix contains only nonzero values for this, we suggest that also S_1^N(LUMO + 1)* and S_1^N(LUMO)* also participate in an interaction with an electron-donating site of the receptor (they do not appear in the equation because their numerical values are constant thorough the family of molecules or because their variation is not statistically significant). Atoms 16 and 20 (a double-bonded oxygen atom) participate through interactions with electron-accepting sites of the receptor. The case of a low numerical value for S_8^N(LUMO + 2)* is interesting. Figure 10 shows the (LUMO + 2)* for atom 8 in molecules 1 and 9 (see Figure 1).

The (LUMO + 2)* shows a strong σ character on atom 8 in both molecules. As it is well known that these kinds of MOs do not participate in charge transfer, the small value for S_8^N(LUMO + 2)* can be interpreted as facilitation for

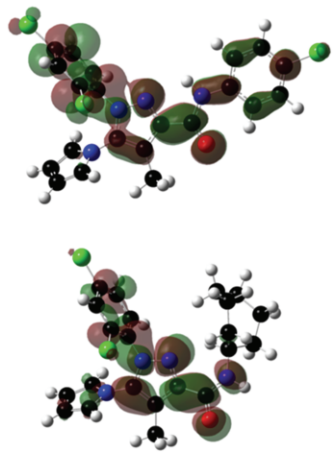

Figure 10: Localization of the $(\text{LUMO} + 2)^*$ for atom 8 in molecules 1 (upper) and 6 (lower) (isovalue = 0.02 e).

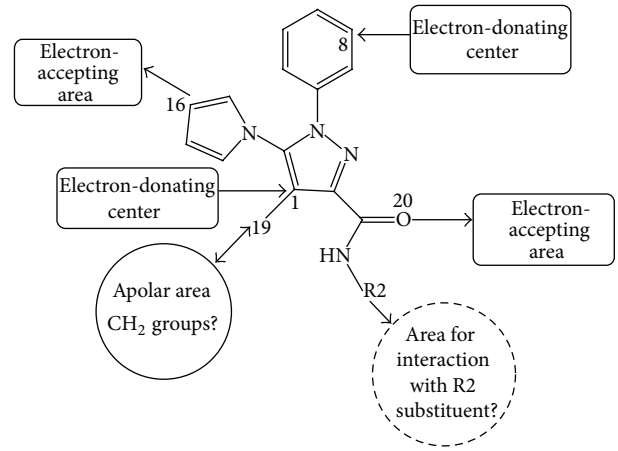

Figure 11: 2D interaction pharmacophore for Set I.

an optimal interaction of $S_8^N(\text{LUMO} + 1)^*$ and $S_8^N(\text{LUMO})^*$ (both having a π character) with an electron-donating center of the receptor. In the case of atom 19, the $(\text{HOMO} - 1)^*$ is of σ character. We interpret a high value of $S_{19}^E(\text{HOMO} - 1)^*$ as the interaction of the methyl group with an apolar area of the hCB1 receptor (probably with lateral methylene chains of amino acids). This last statement is supported by the fact that atom 19 has a high local atomic hardness.

A very important fact is that (10) explains only about 86% of the variation of the hCB1 receptor binding affinity. This strongly suggests that there is an additional sector of this family of molecules that has not been included in this skeleton. Support for this suggestion is provided by Figure 3, spanning two orders of magnitude and showing that there are several molecules falling outside the 95% confidence interval. The MO localization evidence permits us to conjecture that the R2 aromatic substituents are also interacting with the receptor. We did not test this hypothesis because of the problems arising to build the common skeleton for this new area [70]. Another possibility could be the fact that we did not consider more local atomic reactivity indices for the common skeleton [46] such as the local atomic density of states or higher terms of the infinite expansion. This was not done because we are still analyzing their physical meaning. Then, interactions of these molecules are highly specific, being in this case orbital controlled [59]. The set of these interpretations is shown in the two-dimensional (2D) interaction pharmacophore of Figure 11.

For the case of Set II (with saturated R2 substituents) (11) explains about 95% of the variation of the hCB1 receptor binding affinity. This is a satisfactory result and suggests that the R2 substituent is not interacting with a complementary site of the receptor. Using molecules 1 and 6 as examples we may see that the R2 substituents are more or less equal in size but entirely different regarding electronic structure (i.e., in the actual case the R2 substituents have no π electrons). If we accept that in the previous case (Set I) the aromatic R2 substituents interact with a place of the hCB1 receptor through their π electrons, then, in this case, or an area of the receptor should have enough conformational flexibility to accommodate an apolar R2 substituent or the drug molecule adopts a conformation with the R2 substituent pointing in a different direction than in the fully optimized structure (or both possibilities). Table 6 shows that there are no significant correlations between the independent variables. The most relevant variables are $Q_8^{\max}$ and $F_{19}(\text{HOMO} - 2)^*$ (see Table 5). A VBV analysis shows that a high receptor binding affinity is associated with high values for $S_5^E(\text{HOMO} - 2)^*$ and $Q_8^{\max}$ and with small values for $F_{19}(\text{HOMO} - 2)^*$ and Φ_{R1}. Figure 4, spanning three orders of magnitude, shows a good correlation between observed and calculated values. We shall tentatively interpret the requirement of a small value for $F_{19}(\text{HOMO} - 2)^*$ (a σ MO) by suggesting that a great electron population on the $(\text{HOMO} - 2)^*$ of atom 19 (which has a total negative net charge) hinders in some way the interaction with the proposed apolar region for Set I. This is a point that needs more research. The high value required for $S_5^E(\text{HOMO} - 2)^*$ indicates the possible interaction of the three occupied MOs localized on atom 5 with an electron-accepting area of the receptor. The value of $Q^{\max}$ for atom 8 suggests that this atom should be able to receive extra electronic charge from an electron-donating center located on the receptor. This is exactly the same case of Set I (see Figure 11). The low value required for Φ_{R1} is a good example of how H, F, and Cl substitutions may exert a nonelectronic influence on the receptor affinity. As the three atoms produce different effects on the electronic structure of Ring C, the experimentalist should be able to find equilibrium between electronic and orientational effects by testing substitutions having the same electronic effect. This interaction seems to be charge, orbital, and steric controlled. Figure 12 shows the 2D interaction pharmacophore for Set II.

4.2. hCB2 Receptor Binding Results. Table 7 indicates that the order of importance of the variables is $S_{17}^N(\text{LUMO})^* > F_{20}(\text{LUMO} + 2)^* > F_4(\text{LUMO} + 1)^* > Q_{19}$. Table 8 shows that no significant correlation exists among independent variables. Figure 5, spanning two orders of magnitude, shows a good correlation between experimental and calculated

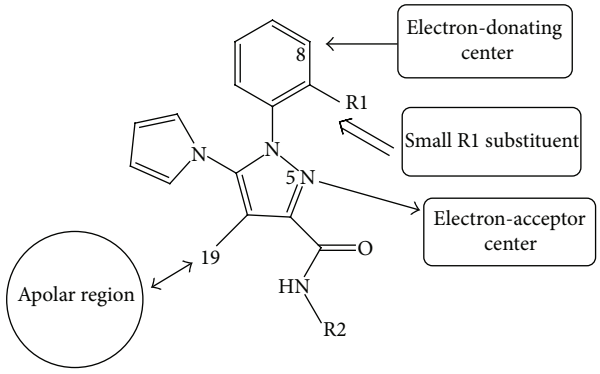

Figure 12: 2D interaction pharmacophore for Set II.

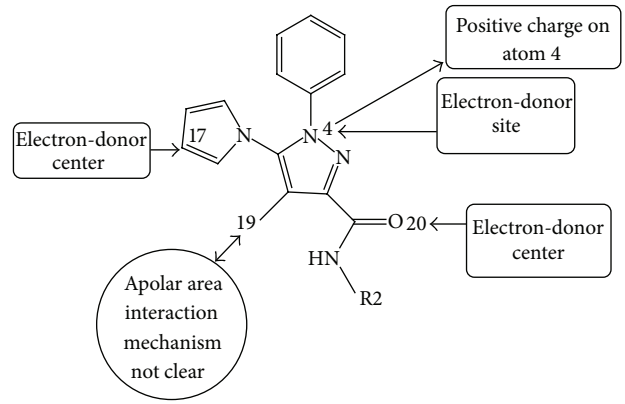

Figure 13: 2D interaction pharmacophore for Set III.

values. Equation (12) (Set III, aromatic R2 substituents) shows that a good binding affinity is associated with large values for $F_{19}(\text{LUMO}+2)^*$ and $F_{20}(\text{LUMO}+2)^*$, negative values for $S^N_{17}(\text{LUMO})^*$, small values for $F_4(\text{LUMO}+1)^*$, and a positive net charge on atom 19. Atom 20 is an oxygen one (Figure 1) and the three highest empty MOs located on it are of π nature. With this data we suggest that this atom is interacting with an electron-donating center of the hCB2 receptor. Atom 19 (the C atom of a methyl group) has a very high local atomic hardness indicating that for it the $\text{HOMO}^* - \text{LUMO}^*$ gap is relatively large hindering it to act as an electron-donating or an electron-accepting center (e.g., μ_{19} is 9.31 eV for molecule 1 and 9.25 eV for molecule 6). Its beta coefficient (Table 6) shows that its contribution to the variation of the hCB2 binding affinity is important. We propose that the methyl group is facing an apolar area such as methylene groups of amino acids. Knowing that (7) is a truncated expression of an infinite series expansion we think that it seems necessary to introduce some terms that could give an account of the interpenetrability of the electron density between two partners. An educated guess points to the local atomic density of states, terms that were not included in this work but that were obtained by us during the development of the general model [46]. The positive net charge on atom 19 suggests an electrostatic interaction with a negative counterpart. A low value for $F_4(\text{LUMO}+1)^*$, a σ MO, suggests that this term acts by obstructing the optimal interaction of $F_4(\text{LUMO})^*$, an MO of π character, with an electron-donating site located in the receptor. A negative value for $S^N_{17}(\text{LUMO})^*$ indicates that this atom (and probably all the aromatic moiety) also interacts with an electron-donor site of the receptor. As (12) explains about 96% of the variation of the hCB2 receptor binding it seems that the aromatic R2 substituents do not interact with an area of this receptor. This interaction is charge and orbital controlled. The corresponding interaction pharmacophore is shown in Figure 13.

For Set IV (saturated R2 substituents), Table 9 indicates that the order of importance of the variables is $\mu_{12} > \Phi_{R2} > F_{12}(\text{HOMO})^* > S^E_{18}(\text{HOMO}-1)^*$. Table 10 shows that there is a correlation of 38% between Φ_{R2} and $F_{12}(\text{HOMO})^*$. Note that Φ_{R2} is a purely geometric index while $F_{12}(\text{HOMO})^*$ is a purely electronic one. Figure 6 shows a good correlation between experimental and calculated values. A VBV analysis shows that a good hCB2 receptor binding affinity is associated with small values for the local atomic electronic chemical potential of atom 7 and $S^E_{18}(\text{HOMO}-1)^*$, and with great values for the orientational parameter of the R2 substituent and possibly for $F_{12}(\text{HOMO})^*$ (13). As this equation explains about 94% of the variation of the hCB2 receptor binding affinity, we think that the R2 substituent does not interact with the hCB2 receptor. This is consistent with the results for Set III. The high value required for the orientational parameter of R2 suggests that this moiety could serve only slowing the rotational velocity of the whole molecule in order to provide enough time for the recognition process. Noting that this term does not appear in the hCB1 cases (Sets I and II) we advance the idea that the in vitro form of the hCB2 receptor site is less accessible than the hCB1 receptor site. The low numerical value required for $S^E_{18}(\text{HOMO}-1)^*$ is consistent with the fact that the $(\text{HOMO}-1)^*$ of atom 18 is of σ character while its $(\text{HOMO})^*$ is of π character. Then, a facilitation of the $(\text{HOMO})^*$ interaction with an electron-accepting site of the receptor will occur with a very small or zero electron population at the $(\text{HOMO}-1)^*$ level. Strictly speaking this can be done by substituting the molecule in such a way that the $(\text{HOMO}-1)^*$ of atom 18 is shifted to inner occupied MOs. A high value for $F_{12}(\text{HOMO})^*$ indicates that this atom is engaged with a receptor site as an electron-donating center. This is totally consistent with the low value required for μ_{12} (low μ values correspond to good electron donors [46]). The interaction pharmacophore for Set IV is shown in Figure 14.

Note finally that if we compare the 2D pharmacophores for Sets I and II we do not observe contradictory facts in them (e.g., a given atom acting as an electron donor in one pharmacophore and as an electron acceptor in the other). The same happens in the pharmacophores for Sets III and IV.

The main conclusions of this work are as follows. (1) We obtained statistically significant equations relating the variation of hCB1 and hCB2 receptor binding affinities with the variation of definite sets of local atomic reactivity indices. (2) The study of the interaction of the molecules with the hCB1 receptors strongly suggests that there is an extra site in

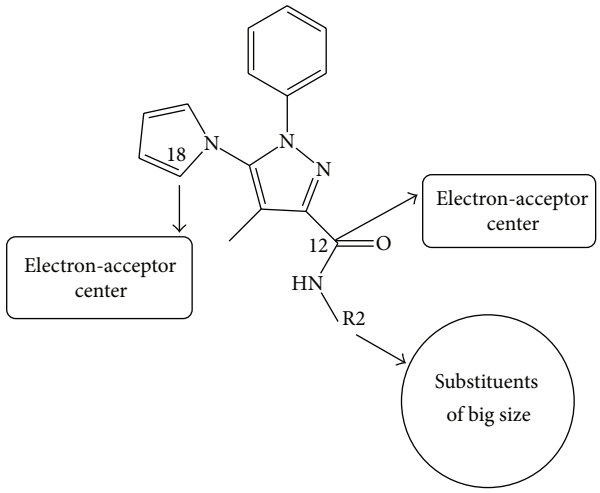

Figure 14: 2D interaction pharmacophore for Set IV.

the receptor that interacts with aromatic R2 substituents. (3) The interaction of the hCB1 receptor with molecules carrying an aromatic R2 substituent seems to be charge-controlled. (4) In the case of molecules having a saturated R2 substituent, their interaction with the hCB1 receptor is orbital, charge and steric controlled. (5) In the case of hCB2 receptors there is no evidence of the existence of an extra site that interacts with aromatic R2 substituents. (6) The interaction of hCB2 receptors with molecules carrying an aromatic substituent at R2 is orbital and charge controlled, while for molecules having a saturated R2 substituent it is orbital and steric controlled.

Conflict of Interests

The authors declare that they have no conflict of interest.

References

[1] E. L. Abel, *Marihuana, the First Twelve Thousand Years*, McGraw-Hill, New York, NY, USA, 1982.

[2] H.-L. Li, "An archaeological and historical account of Cannabis in China," *Economic Botany*, vol. 28, no. 4, pp. 437–448, 1973.

[3] M. L. Ryder, "Probable fibres from hemp (*Cannabis sativa* L.) in bronze age Scotland," *Environmental Archaeology*, vol. 4, no. 1, pp. 93–95, 1999.

[4] C. Sherman, A. Smith, and E. Tanner, *Highlights: An Illustrated History of Cannabis*, Ten Speed Press, Berkeley, Calif, USA, 1999.

[5] J. P. Mallory and V. H. Mair, *The Tarim Mummies: Ancient China and the Mystery of the Earliest Peoples from the West, with 190 illustrations, 13 in color*, Thames & Hudson, New York, NY, USA, 2000.

[6] M. Booth, *Cannabis: A History*, Picador, New York, NY, USA, 2005.

[7] C. Bennett, *Cannabis and the Soma Solution*, TrineDay, Waterville, Ore, USA, 2010.

[8] H.-E. Jiang, X. Li, Y.-X. Zhao et al., "A new insight into *Cannabis sativa* (Cannabaceae) utilization from 2500-year-old Yanghai Tombs, Xinjiang, China," *Journal of Ethnopharmacology*, vol. 108, no. 3, pp. 414–422, 2006.

[9] W. Emboden, "*Cannabis*—a polytypic genus," *Economic Botany*, vol. 28, no. 3, pp. 304–310, 1974.

[10] E. Small, H. D. Beckstead, and A. Chan, "The evolution of cannabinoid phenotypes in Cannabis," *Economic Botany*, vol. 29, no. 3, pp. 219–232, 1975.

[11] E. Small and A. Cronquist, "A practical and natural taxonomy for Cannabis," *Taxon*, vol. 25, no. 4, pp. 405–435, 1976.

[12] E. Small, P. Y. Jui, and L. P. Lefkovitch, "A numerical taxonomic analysis of Cannabis with special reference to species delimitation," *Systematic Botany*, vol. 1, no. 1, pp. 67–84, 1976.

[13] S. L. Datwyler and G. D. Weiblen, "Genetic variation in hemp and marijuana (*Cannabis sativa* L.) according to amplified fragment length polymorphisms," *Journal of Forensic Sciences*, vol. 51, no. 2, pp. 371–375, 2006.

[14] S. Chandra, H. Lata, A. M. Galal, I. A. Khan, and M. A. ElSohly, "Botany of *Cannabis sativa* L.: identification, cultivation and processing," *Planta Medica*, vol. 77, no. 5, article P_4, 2011.

[15] H. van Bakel, J. Stout, A. Cote et al., "The draft genome and transcriptome of *Cannabis sativa*," *Genome Biology*, vol. 12, no. 10, article R102, 2011.

[16] J. H. Mills, *Madness, Cannabis and Colonialism: The "Native Only" Lunatic Asylums of British India, 1857–1900*, St. Martin's Press, New York, NY, USA, 2000.

[17] J. H. Mills, *Cannabis Britannica: Empire, Trade, and Prohibition, 1800–1928*, Oxford University Press, Oxford, UK, 2003.

[18] J. H. Mills and P. Barton, *Drugs and Empires: Essays in Modern Imperialism and Intoxication, c.1500–c.1930*, Palgrave Macmillan, Basingstoke, UK, 2007.

[19] J. S. Gómez-Jeria, F. Soto-Morales, and G. Larenas-Gutierrez, "A zindo/1 study of the cannabinoid-mediated inhibition of adenylyl cyclase," *Iranian International Journal of Science*, vol. 4, no. 2, pp. 151–164, 2003.

[20] J. S. Gómez-Jeria, F. Soto-Morales, J. Rivas, and A. Sotomayor, "A theoretical structure-affinity relationship study of some cannabinoid derivatives," *Journal of the Chilean Chemical Society*, vol. 53, no. 1, pp. 1382–1388, 2008.

[21] C. Hale, *Himmler's Crusade: The Nazi Expedition to Find the Origins of the Aryan Race*, John Wiley & Sons, Hoboken, NJ, USA, 2003.

[22] R. G. Pertwee, "Cannabinoid pharmacology: the first 66 years," *British Journal of Pharmacology*, vol. 147, supplement 1, pp. S163–S171, 2006.

[23] R. G. Pertwee, A. C. Howlett, M. E. Abood et al., "International union of basic and clinical pharmacology. LXXIX: cannabinoid receptors and their ligands: beyond CB_1 and CB_2 ," *Pharmacological Reviews*, vol. 62, no. 4, pp. 588–631, 2010.

[24] L. Console-Bram, J. Marcu, and M. E. Abood, "Cannabinoid receptors: nomenclature and pharmacological principles," *Progress in Neuro-Psychopharmacology and Biological Psychiatry*, vol. 38, no. 1, pp. 4–15, 2012.

[25] N. Battista, M. di Tommaso, M. Bari, and M. Maccarrone, "The endocannabinoid system: an overview," *Frontiers in Behavioral Neuroscience*, vol. 6, article 9, 2012.

[26] F. Pamplona and R. Takahashi, "Psychopharmacology of the endocannabinoids: far beyond anandamide," *Journal of Psychopharmacology*, vol. 26, no. 1, pp. 7–22, 2012.

[27] R. Mechoulam and L. A. Parker, "The endocannabinoid system and the brain," *Annual Review of Psychology*, vol. 64, no. 1, pp. 21–47, 2013.

[28] E. J. van Bockstaele, "Endocannabinoids and monoamines: modulating the modulators," in *Endocannabinoid Regulation of Monoamines in Psychiatric and Neurological Disorders*, E. J. van Bockstaele, Ed., pp. 1–9, Springer, New York, NY, USA, 2013.

[29] R. A. Archer, D. B. Boyd, P. V. Demarco, I. J. Tyminski, and N. L. Allinger, "Structural studies of cannabinoids. Theoretical and proton magnetic resonance analysis," *Journal of the American Chemical Society*, vol. 92, no. 17, pp. 5200–5206, 1970.

[30] E. A. Carlini, M. Santos, U. Claussen, D. Bieniek, and F. Korte, "Structure activity relationship of four tetrahydrocannabinols and the pharmacological activity of five semi-purified extracts of *Cannabis sativa*," *Psychopharmacologia*, vol. 18, no. 1, pp. 82–93, 1970.

[31] H. Edery, Y. Grunfeld, Z. Ben-Zvi, and R. Mechoulam, "Structural requirements for cannabinoid activity," *Annals of the New York Academy of Sciences*, vol. 191, no. 1, pp. 40–53, 1971.

[32] B. Loev, P. E. Bender, F. Dowalo, E. Macko, and P. J. Fowler, "Cannabinoids. Structure-activity studies related to 1,2-dimethylheptyl derivatives," *Journal of Medicinal Chemistry*, vol. 16, no. 11, pp. 1200–1206, 1973.

[33] D. B. Uliss, H. C. Dalzell, G. R. Handrick, J. F. Howes, and R. K. Razdan, "Hashish. Importance of the phenolic hydroxyl group in tetrahydrocannabinols," *Journal of Medicinal Chemistry*, vol. 18, no. 2, pp. 213–215, 1975.

[34] P. F. Osgood, J. F. Howes, R. K. Razdan, and H. G. Pars, "Drugs derived from cannabinoids. 7: tachycardia and analgesia structure-activity relationships in Δ9-tetrahydrocannabinol and some synthetic analogues," *Journal of Medicinal Chemistry*, vol. 21, no. 8, pp. 809–811, 1978.

[35] S. H. Smith, L. S. Harris, I. M. Uwaydah, and A. E. Munson, "Structure-activity relationships of natural and synthetic cannabinoids in suppression of humoral and cell-mediated immunity," *Journal of Pharmacology and Experimental Therapeutics*, vol. 207, no. 1, pp. 165–170, 1978.

[36] T. Cordova, D. Ayalon, N. Lander et al., "The ovulation blocking effect of cannabinoids: structure-activity relationships," *Psychoneuroendocrinology*, vol. 5, no. 1, pp. 53–62, 1980.

[37] I. Tamir, R. Mechoulam, and A. Y. Meyer, "Cannabidiol and phenytoin: a structural comparison," *Journal of Medicinal Chemistry*, vol. 23, no. 2, pp. 220–223, 1980.

[38] F. Hucho, *Neuroreceptors: Proceedings of the Symposium, Berlin (West), September 28-29, 1981*, Walter de Gruyter, Berlin, Germany, 1981.

[39] B. R. Martin, M. J. Kallman, G. F. Kaempf, L. S. Harris, W. L. Dewey, and R. K. Razdan, "Pharmacological potency of R- and S-3′-hydroxy-Δ9-tetrahydrocannabinol: additional structural requirement for cannabinoid activity," *Pharmacology Biochemistry and Behavior*, vol. 21, no. 1, pp. 61–65, 1984.

[40] R. K. Razdan, "Structure-activity relationships in cannabinoids," *Pharmacological Reviews*, vol. 38, no. 2, pp. 75–149, 1986.

[41] R. S. Rapaka and A. Makriyannis, *Structure-Activity Relationships of the Cannabinoids*, U.S. Department of Health and Human Services, Public Health Service, Alcohol, Drug Abuse, and Mental Health Administration, Rockville, Md, USA, 1987.

[42] R. Silvestri, A. Ligresti, G. L. Regina et al., "Synthesis, cannabinoid receptor affinity, molecular modeling studies and in vivo pharmacological evaluation of new substituted 1-aryl-5-(1H-pyrrol-1-yl)-1H-pyrazole-3-carboxamides. 2. Effect of the 3-carboxamide substituent on the affinity and selectivity profile," *Bioorganic & Medicinal Chemistry*, vol. 17, no. 15, pp. 5549–5564, 2009.

[43] J. S. Gomez Jeria, "La pharmacologie quantique," *Bollettino Chimico Farmaceutico*, vol. 121, no. 12, pp. 619–625, 1982.

[44] J. S. Gómez-Jeria, "On some problems in quantum pharmacology I. The partition functions," *International Journal of Quantum Chemistry*, vol. 23, no. 6, pp. 1969–1972, 1983.

[45] J. S. Gómez-Jeria, "Modeling the drug-receptor interaction in quantum pharmacology," in *Molecules in Physics, Chemistry, and Biology*, J. Maruani, Ed., vol. 4, pp. 215–231, Springer, Amsterdam, The Netherlands, 1989.

[46] J. S. Gómez-Jeria, "A new set of local reactivity indices within the Hartree-Fock-Roothaan and density functional theory frameworks," *Canadian Chemical Transactions*, vol. 1, no. 1, pp. 25–55, 2013.

[47] J. S. Gómez-Jeria and D. R. Morales-Lagos, "Quantum chemical approach to the relationship between molecular structure and serotonin receptor binding affinity," *Journal of Pharmaceutical Sciences*, vol. 73, no. 12, pp. 1725–1728, 1984.

[48] J. S. Gómez-Jeria, D. Morales-Lagos, J. I. Rodriguez-Gatica, and J. C. Saavedra-Aguilar, "Quantum-chemical study of the relation between electronic structure and pA_2 in a series of 5-substituted tryptamines," *International Journal of Quantum Chemistry*, vol. 28, no. 4, pp. 421–428, 1985.

[49] J. S. Gómez-Jeria, D. Morales-Lagos, B. K. Cassels, and J. C. Saavedra-Aguilar, "Electronic structure and serotonin receptor binding affinity of 7-substituted tryptamines QSAR of 7-substituted tryptamines," *Quantitative Structure-Activity Relationships*, vol. 5, no. 4, pp. 153–157, 1986.

[50] J. S. Gómez-Jeria and P. Sotomayor, "Quantum chemical study of electronic structure and receptor binding in opiates," *Journal of Molecular Structure*, vol. 166, pp. 493–498, 1988.

[51] J. S. Gómez-Jeria, M. Ojeda-Vergara, and C. Donoso-Espinoza, "Quantum-chemical structure-activity relationships in carbamate insecticides," *Molecular Engineering*, vol. 5, no. 4, pp. 391–401, 1995.

[52] J. S. Gómez-Jeria and L. Lagos-Arancibia, "Quantum-chemical structure-affinity studies on kynurenic acid derivatives as Gly/NMDA receptor ligands," *International Journal of Quantum Chemistry*, vol. 71, no. 6, pp. 505–511, 1999.

[53] J. S. Gómez-Jeria, L. A. Gerli-Candia, and S. M. Hurtado, "A structure-affinity study of the opioid binding of some 3-substituted morphinans," *Journal of the Chilean Chemical Society*, vol. 49, no. 4, pp. 307–312, 2004.

[54] F. Soto-Morales and J. S. Gómez-Jeria, "A theoretical study of the inhibition of wild-type and drug-resistant HTV-1 reverse transcriptase by some thiazolidenebenzenesulfonamide derivatives," *Journal of the Chilean Chemical Society*, vol. 52, no. 3, pp. 1214–1219, 2007.

[55] J. S. Gómez-Jeria, "A DFT study of the relationships between electronic structure and peripheral benzodiazepine receptor affinity in a group of N,N-dialkyl-2-phenylindol-3-ylglyoxylamides," *Journal of the Chilean Chemical Society*, vol. 55, no. 3, pp. 381–384, 2010, Erratum in *Journal of the Chilean Chemical Society*, vol. 55, no. 4, p. 9, 2010.

[56] T. Bruna-Larenas and J. S. Gómez-Jeria, "A DFT and semiempirical model-based study of opioid receptor affinity and selectivity in a group of molecules with a morphine structural core," *International Journal of Medicinal Chemistry*, vol. 2012, Article ID 682495, 16 pages, 2012.

[57] R. F. Hudson and G. Klopman, "A general perturbation treatment of chemical reactivity," *Tetrahedron Letters*, vol. 8, no. 12, pp. 1103–1108, 1967.

[58] G. Klopman and R. F. Hudson, "Polyelectronic perturbation treatment of chemical reactivity," *Theoretica Chimica Acta*, vol. 8, no. 2, pp. 165–174, 1967.

[59] G. Klopman, "Chemical reactivity and the concept of charge- and frontier-controlled reactions," *Journal of the American Chemical Society*, vol. 90, no. 2, pp. 223–234, 1968.

[60] K. Fukui and H. Fujimoto, *Frontier Orbitals and Reaction Paths: Selected Papers of Kenichi Fukui*, World Scientific, River Edge, NJ, USA, 1997.

[61] J. S. Gómez-Jeria, *Elements of Molecular Electronic Pharmacology*, Ediciones Sokar, Santiago, Chile, 2013 (Spanish).

[62] D. A. Alarcón, F. Gatica-Díaz, and J. S. Gómez-Jeria, "Modeling the relationships between molecular structure and inhibition of virus-induced cytopathic effects. Anti-HIV and anti-H1N1 (Influenza) activities as examples," *Journal of the Chilean Chemical Society*, vol. 58, no. 3, pp. 1651–1659, 2013.

[63] J. S. Gómez-Jeria and M. Ojeda-Vergara, "Parametrization of the orientational effects in the drug-receptor interaction," *Journal of the Chilean Chemical Society*, vol. 48, no. 4, pp. 119–124, 2003.

[64] J. S. Gómez-Jeria and M. Ojeda-Vergara, "Electrostatic medium effects and formal quantum structure-activity relationships in apomorphines interacting with D_1 and D_2 dopamine receptors," *International Journal of Quantum Chemistry*, vol. 61, no. 6, pp. 997–1002, 1997.

[65] C. Barahona-Urbina, S. Nuñez-Gonzalez, and J. S. Gómez-Jeria, "Model-based quantum-chemical study of the uptake of some polychlorinated pollutant compounds by Zucchini subspecies," *Journal of the Chilean Chemical Society*, vol. 57, no. 4, pp. 1497–1503, 2012.

[66] M. J. Frisch, G. W. Trucks, H. B. Schlegel et al., *Gaussian 98 Rev.A.11.3*, Gaussian, Pittsburgh, Pa, USA, 2002.

[67] J. S. Gómez-Jeria, "An empirical way to correct some drawbacks of mulliken population analysis," *Journal of the Chilean Chemical Society*, vol. 54, no. 4, pp. 482–485, 2009, Erratum in *Journal of the Chilean Chemical Society*, vol. 55, no. 4, p. 9, 2010.

[68] StatSoft, *Statistica 8.0*, StatSoft, Tulsa, Okla, USA, 1984–2007.

[69] J. S. Gómez-Jeria, "Approximate molecular electrostatric potentials of protonated mescaline analogues," *Acta Sud Americana de Química*, vol. 4, no. 1, pp. 1–9, 1984.

[70] J. S. Gómez-Jeria and D. Morales-Lagos, "The mode of binding of phenylalkylamines to the serotonergic receptor," in *QSAR in Design of Bioactive Drugs*, M. Kuchar, Ed., pp. 145–173, Prous, Barcelona, Spain, 1984.